14th IEA Heat Pump Conference
15-18 May 2023, Chicago, Illinois

Exploration of Heat-Driven Ejector High-Temperature Heat Pumps

Pengtao Wang, Stephen Kowalski, Cheng-Min Yang, Jian Sun, Zhiming Gao, Kashif Nawaz*

Multifunctional Equipment Integration Group, Building Technology Research and Integration Center, Oak Ridge National Laboratory, Oak Ridge, TN 37830, USA

Abstract

Heat-driven ejector heat pumps use a supersonic ejector as a thermo-compressor to replace the mechanical compressor. Supersonic ejectors have many advantages in high-temperature heat pump (HTHP) applications, including high operating temperature tolerance, no need for lubrication, low maintenance, and low cost. The coefficient of performance of ejector HTHPs could be improved by selecting binary fluids with unique thermodynamic properties. Although supersonic ejectors have been widely used in refrigeration systems, their application in spaces and water heating is limited. This study explores the theoretical potential of ejector HTHPs with a sink temperature of 100°C–130°C and a lift temperature of 10°C–30°C. Ejector HTHPs were evaluated with single-fluid ejectors (SFEs) and binary-fluid ejectors (BFEs). A comprehensive, geometry-free theoretical model of BFEs was developed to predict the theoretical maximum entrainment ratios. HFE7500 and R718 (water) were selected as working fluids for SFEs and BFEs. SFEs operating with R718 provided a higher coefficient of performance of ejector HTHPs than SFEs operating with HFE7500 and BFEs. This study preliminarily demonstrates the technical potential of ejector HTHP applications in recovering moderate-temperature heat sources.

Selection and/or peer-review under the responsibility of the organizers of the 14th IEA Heat Pump Conference 2023.

Keywords: Ejector, High temperature heat pump, binary fluid, COP;

1. Introduction

High-temperature heat pumps (HTHPs) have great potential to improve energy efficiency and reduce CO_2 emissions by replacing gas-fired boilers for industrial process heating. Many HTHPs under development and case demonstrations operate with electricity-driven vapor compression cycles, as reported by International Energy Agency (IEA) Annex 58. A basic configuration of HTHPs working with a vapor compression cycle is shown in Fig. 1(a), in which a mechanical compressor is used to lift the pressure of the refrigerant vapor (Process 1→2). The compressor is the main component in electric-driven HTHPs, accounting for 48.2%–

* Corresponding author. Tel.: +1-865-241-0972; fax: +0-000-000-0000 .
E-mail address: nawazk@ornl.gov.

57.3% of the total cost of 100 kW HTHPs using R245fa [1]. Corresponding to a high sink temperature (T_{sink} > 100°C) in HTHPs, the high pressure and temperature of refrigerants challenge state-of-the-art compressor technologies in the following ways:

- Risk of wet compression: Emerging refrigerants with a low global warming potential (GWP), such as R1336mzz(Z), have a saturated vapor curve with a positive slope ($\frac{dT}{ds}$), requiring internal heat exchangers to provide substantial superheating of suction vapor [2].
- Overheating of compressors: Auxiliary cooling technology and components are used in HTHPs to effectively control the temperature of compressors, such as the vapor injection technique with an economizer [3].
- Availability of lubricant oils: High temperature and pressure challenge the thermal stability of lubricant oil and its material compatibility with refrigerants and sealing materials [4].
- Limited drop-in operation with alternative refrigerants: Mechanical compressors have complex designs, infrastructure, and process controls [5], making it difficult to operate with various refrigerants.

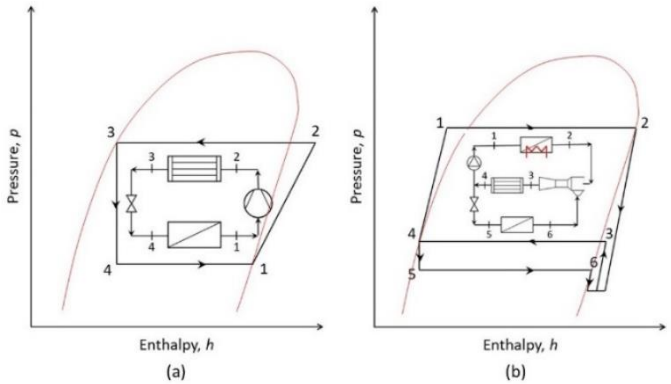

Fig. 1. Schematic of thermodynamic cycles of HTHPs.
(a) Mechanical compressor and (b) ejector thermocompressor.

These challenges associated with electric-driven HTHPs could be alleviated by using heat-driven heat pumps [6]. Heat-driven heat pumps use thermal chemical and physical processes, such as adsorption or absorption HTHPs and transformers; thermal engines, such as Stirling engines and Vuilleumier engines; thermal acoustic coupling effects [7]; and thermo-compressors. The ejector-based HTHP is a typical heat-driven heat pump that uses a supersonic ejector as a thermo-compressor, which replaces the mechanical compressor in a conventional vapor compression cycle, as shown in Fig. 1(b). Primary fluid (PF), at high temperature and pressure (state point 2), accelerates into a supersonic flow and creates a vacuum in the suction chamber of the ejector, which entrains the secondary fluid (SF), at low temperature and pressure (state point 6), into the ejector. PF and SF mix, and the pressure of mixed PF-SF is sequentially lifted to a moderate level (state point 3) through a normal shock wave and a diffusing process. Supersonic ejectors are desirable in HTHPs because of their simple structure, high reliability, low cost, and low maintenance (without moving parts) [8-10]. Furthermore, the ejector could operate with a wide range of refrigerants via drop-in replacement [11], and it is scalable to large systems and multi-stage systems at high temperatures. For example, a steam ejector used in a thermal power plant, driven with a PF at 4.33 MPa and 350°C, could upgrade the low-pressure SF from 1.152 MPa and 400°C to 1.3 MPa and 366°C [12].

Supersonic ejectors in heat-driven refrigeration applications have been extensively studied, and they are attractive for using available waste heat [13] and solar thermal energy [14]. However, few studies have examined ejector-based heat pumps. The technical barriers in ejector-based heat pumps are a low heating cycle coefficient of performance (COP), a small pressure lift ratio, and poor performance under off-design conditions. Theoretically, a low heating cycle COP of ejector heat pumps could be addressed by replacing a single fluid with a binary-fluid pair (i.e., a PF and SF with unique thermal properties) [15]. The heating cycle COP of heat pumps with a binary-fluid ejector (BFE) is approximate to [16, 17]

$$COP_{\mathrm{HP}} = 1 + \omega \frac{\Delta h_{SF}}{\Delta h_{PF}} \approx 1 + \omega \frac{h_{lv,SF}}{\Delta h_{sh,PF} + h_{lv,PF}} \quad (1)$$

where $h_{lv,PF}$ and $h_{lv,SF}$ are the latent heat of evaporation of the PF and the SF, respectively. $\Delta h_{sh,PF}$ is the increased sensible heat of the PF in the high-temperature evaporator (HTE). The entrainment ratio, ω, is defined as the ratio of mass flow rates of the SF and PF, denoted by $\dot{m}_{SF}$ and $\dot{m}_{PF}$.

$$\omega = \frac{\dot{m}_{SF}}{\dot{m}_{PF}} \quad (2)$$

Equation (1) shows that choosing an SF with a larger h_{lv} than PF, and a PF-SF pair yielding a large ω in BFEs, could significantly increase COP_{HP} [18]. Previous theoretical research demonstrated that, for an ejector heat pump water heater with ΔT_{sink} = 65°C, using a binary-fluid pair of HFE7500 and water, $\frac{h_{lv,SF}}{h_{lv,PF}} \approx 25.1$, and neglecting Δh_{PF}, the heating cycle COP could reach 2.0 with a low entrainment ratio of 0.1 [16].

This study explored the technical potential of supersonic ejectors for heat-driven HTHPs operated with T_{sink} = 100°C–130°C and ΔT_{lift} = 10°C–30°C. The single-fluid ejector (SFE) and BFE were theoretically evaluated for the performance of HTHPs. The entrainment ratios of SFEs and BFEs were theoretically predicted with a comprehensive, geometry-free model of an ejector. HFE7500 and R718 (water) are selected as the working fluids for SFE or BFE. The performance of ejectors and ejector HTHPs are investigated for various working conditions.

2. Thermodynamic Model of Heat-driven Ejector HTHPs

A heat-driven ejector HTHP essentially consists of a HTE, a low-temperature evaporator (LTE), an ejector (EJT), a condenser (COND), a separator (SEP), an expansion valve, and a circulation pump, as shown in Fig. 2(a). In Fig. 2, "1, 2, 3, . . ." and "i, ii, iii, . . ." denote the state points in the system-level loop of the HTHP and the component-level process within the EJT, respectively. The working fluid loops are as follows:

1→2, the liquid PF evaporates in the HTE;

i(2)→iii, the high-pressure PF steam accelerates into a supersonic flow and creates a vacuum in the suction chamber of the EJT;

iii→vi←v, PF and SF mix in the constant section of the mixing chamber of the EJT;

vi→vii, the supersonic flow of the mixed PF-SF flows through a normal shock wave;

vii→viii, the subsonic flow of the mixed PF-SF diffuses in the diffuser section of the EJT;

3(viii)→4, the mixed PF-SF vapor condenses in the COND;

4→5 and 5→6, the liquid PF and SF are separated in the SEP;

5→1, the liquid PF is pumped to the HTE;

6→7, the liquid SF throttles in the expansion valve;

7→8, the SF evaporates in the LTE.

iv(8)→v, the SF vapor accelerates into a sonic flow within the EJT.

The EJT in the investigated ejector HTHP could be an SFE or BFE, depending on the selected PF and SF. For the BFE, the separation of PF-SF in the SEP could be a gravity-driven process for an immiscible fluid pair with a large difference in density, or a thermal-driven fractional condensation process for a miscible fluid pair with a large difference in normal boiling point [19]. In this study, a gravity-driven separator was employed for the binary-fluid pair of HFE7500 and R718, as discussed in the following section. If the same working fluid is selected for the PF and SF, the BFE is reduced to the SFE, and the SEP is not needed.

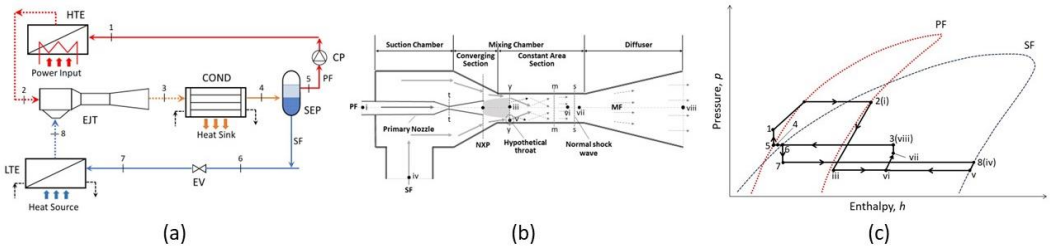

Fig. 2. Schematic of a heat-driven ejector HTHP.
(a) System configuration, (b) gas-dynamic process within an ejector [20], and (c) pressure–enthalpy diagram.

2.1. Thermodynamic Model of an Ejector HTHP

A thermodynamic model of a two-stage BFE HPWH was developed by applying the mass and energy conservation for each component, as summarized in Table 1 [16, 20, 21]. The operating parameters specified for the ejector-drive HTHPs include the sink temperature, T_{sink}, the source temperature, T_{source}, and the driven temperature, T_{HTE}. T_{sink} is the temperature of heat delivered by HTHPs, and $T_{\text{sink}} = T_{\text{COND}}$. T_{source} is the temperature of waste heat available for HTHPs, and $T_{\text{source}} = T_{\text{LTE}}$. The lift temperature of HTHP, ΔT_{lift}, is defined as

$$\Delta T_{lift} = T_{\text{sink}} - T_{\text{source}} = T_{\text{COND}} - T_{\text{LTE}} \tag{3}$$

The system-level performance of an ejector HPWH was evaluated by its heating cycle COP, COP_{HP}, given as

$$COP_{HP} = \frac{Q_{\text{COND}}}{Q_{\text{HTE}}} \approx 1 + \frac{Q_{\text{LTE}}}{Q_{\text{HTE}}} \tag{4}$$

where Q_{COND} is the thermal capacity of the ejector HTHP, which equals the released heat of the mixed PF-SF discharged from the ejector. Q_{HTE} and Q_{LTE} are the heat input in the HTE and the LTE, respectively.

Table 1. The mass and energy equations in the thermodynamic model of the BFE HTHP

Components	Working fluid	Mass equations	Energy equations	Thermal properties equations
HTE	PF	$\dot{m}_1 = \dot{m}_2 = \dot{m}_{PF}$	$Q_{HTE} = \dot{m}_1(h_2 - h_1)$	$h_2 = h(PF, T_2, x = 1)$ $T_2 = T_{HTE}$ $h_1 = h_5$
LTE	SF	$\dot{m}_7 = \dot{m}_8 = \dot{m}_{SF}$	$Q_{LTE} = \dot{m}_8(h_8 - h_7)$	$h_8 = h(SF, T_8, x = 1)$ $T_8 = T_{source}$ $= T_{sin\,k} - \Delta T_{lift}$ $h_7 = h_6$
EJT	PF-SF	$\dot{m}_3 = \dot{m}_2 + \dot{m}_8$	$\dot{m}_3 h_3 = \dot{m}_2 h_2 + \dot{m}_8 h_8$	—
COND	PF-SF	$\dot{m}_4 = \dot{m}_3 = \dot{m}_2 + \dot{m}_8$	$Q_{COND} = \dot{m}_2(h_3 - h_{4,PF}) + \dot{m}_8(h_3 - h_{4,SF})$	$h_{4,PF} = h(PF, T_4, x = 0)$ $h_{4,SF} = h(SF, T_4, x = 0)$ $T_4 = T_{\text{sink}}$
SEP	PF-SF	$\dot{m}_5 = \dot{m}_{PF}$ $\dot{m}_6 = \dot{m}_{SF}$	—	$h_5 = h_{4,PF}$ $h_6 = h_{4,SF}$
EV	SF	$\dot{m}_7 = \dot{m}_6$	—	$h_7 = h_6$
CP	PF	$\dot{m}_1 = \dot{m}_5$	$W = \frac{1}{\eta_{PM}} \frac{\dot{m}_5(p_1 - p_5)}{\rho_5}$ and $\eta_{PM} = 0.5$ $h_1 = h_5 + \frac{W}{\dot{m}_1}$	$\rho_5 = \rho(PF, T_5, x = 0)$ $p_5 = p(PF, T_5, x = 0)$ $p_1 = p(PF, T_1, x = 0)$ $T_5 = T_4$

For the investigated ejector HTHP with a specified thermal capacity, the mass flow rates of the PF and SF were predicted by a theoretical model of the BFE. The comprehensive, geometry-free model predicted the

optimized performance of ejectors under specified operating parameters of HTHPs. The theoretical model was developed based on the gas-dynamic equations and the conservation equations [22, 23]. Detailed information of the theoretical model of the BFE was reported in previous publications [20, 21]. The theoretical model of the BFE was solved with the real properties of working fluids using the Engineering Equation Solver (EES, F-Chart software). The model predicted the theoretical maximum value of ω for an ejector operated under on-design conditions [21]. It is assumed that

- The isentropic efficiencies of ejector components in the theoretical model include 0.92 for the primary nozzle, 0.86 for the secondary nozzle, 0.95 for the mixing chamber, and 0.81 for the diffuser [15];
- The PF and SF entering the ejector are saturated vapor at T_{HTE} and T_{LTE}, respectively; and
- The critical backpressure of the ejector is the saturated vapor pressure of the mixed PF-SF (in a two-phase condition) at T_{COND}.

3. Working Fluids for Heat-driven Ejector HTHPs

The performance of an ejector is closely related to the ejector's backpressure, which equals the saturated vapor pressure of the working fluid in the COND. For an ejector with a fixed geometry, its optimum performance could be achieved under on-design conditions, which require the backpressure to be no larger than the ejector's critical backpressure. For the heat-driven ejector HTHPs in this study, high normal boiling points corresponding to low saturated vapor pressure at T_{sink} were prioritized in selecting the working fluids. Additional considerations in selecting binary-fluid pairs included the following:

- The PF has a much larger molecular weight (*MW*) than the SF for a high entrainment ratio of BFEs;
- The SF has a much larger latent heat of evaporation for a high COP of HTHPs; and
- The PF and SF are immiscible and have significant different density for gravity-driven separation; or the PF and SF have a significant difference in normal boiling point (*NBP*) for thermal separation.

HFE7500 and R718 were selected as the working fluids, as described in Table 2. HFE7000 is a hydrofluoroether (HFE) with a relatively low GWP and zero ozone depletion potential. HFEs are nonflammable fluids with low toxicity, are chemically inert, and have high-temperature stability [24]. HFEs are considered to be third-generation refrigerants to replace chlorofluorocarbons, hydrochlorofluorocarbons, and hydrofluorocarbons [25].

R718 is a natural refrigerant that has been extensively used in ejector-based refrigeration systems. The challenges of using R718 in HTHPs are high compression ratio, large adiabatic coefficient, and low vapor density. Therefore, large-scale multi-stage compressors with intermediate cooling are required in conventional HTHPs. R718 is an ideal working fluid for ejector HTHPs because of the large latent heat of evaporation, high critical temperature, and relatively low vapor pressure at T_{sink}.

Table 2. Working fluids for heat-driven ejector HTHPs

Fluid	Formula	*MW*	*NBP* (°C)	T_{cr} (°C)	P_{cr} (MPa)	h_{lv}* (kJ/kg)	GWP	Group
HFE7500	$C_9H_5F_{15}O$	414	128.4	261.0	1.55	84.0 at 140°C	90	HFE
R718	H_2O	18	99.97	373.9	22.064	2,333.0 at 70°C	0	Natural

4. Performance of Heat-driven Ejector HTHPs

The investigated ejector HTHP was operated with T_{sink} = 100°C–130°C and ΔT_{lift} = 10°C–30°C. The temperature difference for heat transfer in the COND and the LTE was neglected. The inlet of the SF and the discharged PF-SF mixture for the ejector were saturated vapor at T_{LTE} and T_{COND}, respectively. The inlet of the PF is saturated vapor at the operating temperature of T_{HTE}, which is a variable parameter in a range of 190°C–260°C. The maximum pressure of HTE, $P_{\text{HTE,max}}$, is 4.7 MPa for R718 and 1.5 MPa for HFE7500. The theoretical model of the ejector predicted the entrainment ratio, ω, with the inlet and outlet conditions of the working fluids. The performance of the ejector HTHP was evaluated with a unit mass flow rate of PF (1 kg/s), which corresponds to an SF mass flow rate of ω kg/s.

4.1. BFEs and BFE HTHPs

The BFE operated with HFE7500 as the PF and R718 as the SF. Figure 3 shows the component-level performance of BFEs, ω_{BFE}, and the system-level performance of BFE HTHPs, COP_{HP}, under various T_{HTE} and ΔT_{lift}. For a specified ΔT_{lift}, ω_{BFE} increased as T_{HTE} increased until ω_{BFE} reached its maximum value, $\omega_{BFE,max}$; after that, further increasing T_{HTE} significantly reduced ω_{BFE}. The existing optimum temperature of HTE, $T_{HTE,opt}$, for $\omega_{BFE,max}$ was consistent with previous experimental and theoretical results of SFEs in heat-driven refrigeration systems [26] and ejector heat pump water heaters [20, 27]. $T_{HTE,opt}$ is related to the critical points of the PF, T_{cr}, as the thermal physical property of the PF significantly deteriorates near its critical point. For HFE7500 with T_{cr} = 261.0°C, $T_{HTE,opt}$ = 240°C. For a specified T_{sink}, ΔT_{lift} had no obvious effects on $T_{HTE,opt}$ because ΔT_{lift} was only related to the inlet condition of the SF. The trends of COP_{HP} vs. T_{HTE} and ΔT_{lift} were similar to those of ω_{BFE}, indicating that ω_{BFE} dominated the performance of ejector HTHPs. For T_{sink} = 120°C, as ΔT_{lift} increased from 10°C to 30°C, $\omega_{BFE,max}$ decreased from 0.12 to 0.05, and $COP_{HP,max}$ decreased from 2.14 to 1.43.

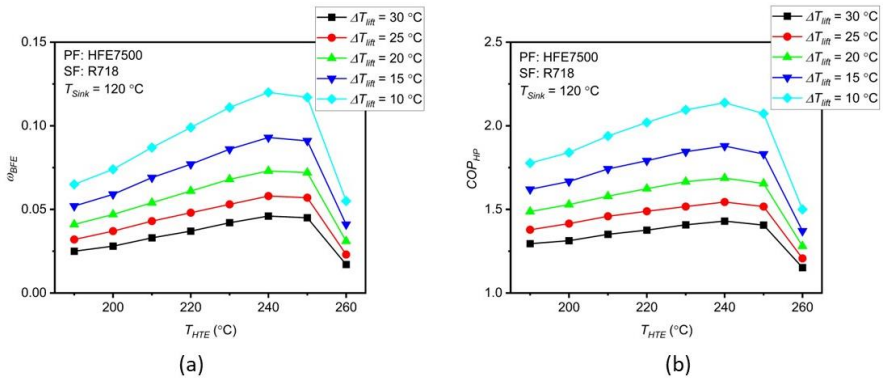

Fig. 3. Typical performance of BFEs and BFE HTHPs. (a) Entrainment ratio and (b) COP.

Figure 4 shows $\omega_{BFE,max}$ and $COP_{HP,max}$ vs. ΔT_{lift} with various T_{sink}. Generally, higher ΔT_{lift} and/or T_{sink} result in lower $\omega_{BFE,max}$ and $COP_{HP,max}$, and the influences of T_{sink} weaken at higher ΔT_{lift}. The largest values of $\omega_{BFE,max}$ and $COP_{HP,max}$ were 0.16 and 2.48, achieved at ΔT_{lift} = 10°C and T_{sink} = 110°C. The smallest values of $\omega_{BFE,max}$ and $COP_{HP,max}$ were 0.04 and 1.39, achieved at ΔT_{lift} = 30°C and T_{sink} = 130°C. Regarding the thermo-compressor, the ejector increased the low pressure of the SF vapor (i.e., $p_{sat,SF}$ at T_{evap}) to moderate pressure (i.e., $p_{sat,SF}$ at T_{sink}). For a specified T_{sink}, a higher ΔT_{lift} provided a lower vapor pressure of the SF entering the BFE. For a specified ΔT_{lift}, a higher T_{sink} required a higher vapor pressure of the SF discharged from the BFE. Therefore, higher ΔT_{lift} and/or T_{sink} consumed more power provided by the kinetic energy of the PF, resulting in lower energy efficiencies of BFEs and HTHPs.

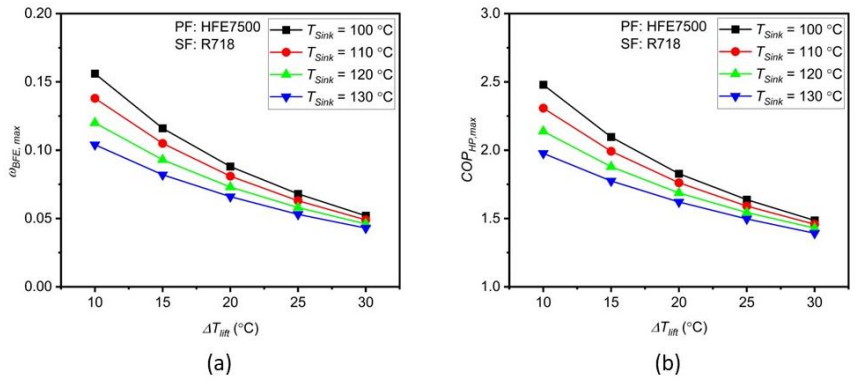

Fig. 4. The maximum performance of BFEs and BFE HTHPs. (a) Maximum entrainment ratio and (b) maximum COP.

4.2. SFEs and SFE HTHPs

The $T_{HTE,opt}$ for the maximum performance of SFEs and SFE HTHPs was 230°C for HFE7500 and 260°C for R718. Figures 5 and 6 show the performance of SFEs and SFE HTHPs operating with HFE7500 and R718, respectively. Similar to BFEs, higher ΔT_{lift} and/or T_{sink} result in lower $\omega_{SFE,max}$ and $COP_{HP,max}$. However, the influences of T_{sink} on $\omega_{SFE,max}$ and $COP_{HP,max}$ were less sensitive than those of BFEs, particularly for HFE7500 at higher ΔT_{lift}, and for R718. SFEs with HFE7500 had higher $\omega_{SFE,max}$ than SFEs with R718 because of the much higher molecular weight of HFE7500 than R718 [28]. However, HFE7500 provided lower $COP_{HP,max}$ than R718. For HFE7500, the largest value of $\omega_{SFE,max}$ was 2.86, and the largest value of $COP_{HP,max}$ was 2.14, achieved at ΔT_{lift} = 10°C and T_{sink} = 130°C. For R718, the largest value of $\omega_{SFE,max}$ was 1.771, and the largest values of $COP_{HP,max}$ was 2.67, also achieved at ΔT_{lift} = 10°C and T_{sink} = 130°C.

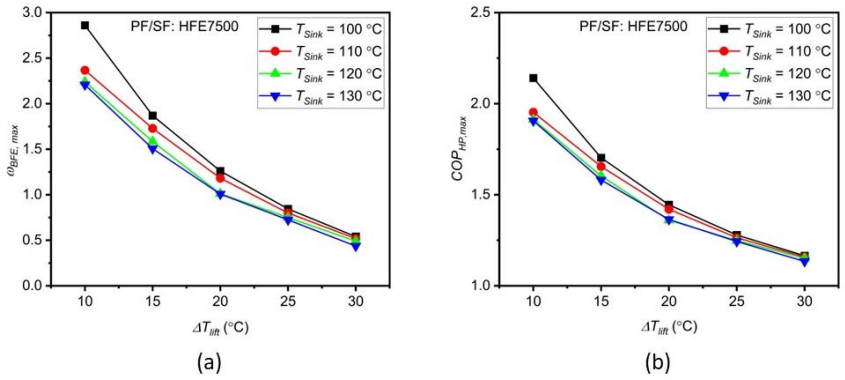

Fig. 5. The maximum performance of SFEs and SFE HTHPs with HFE7500. (a) Maximum entrainment ratio and (b) maximum COP.

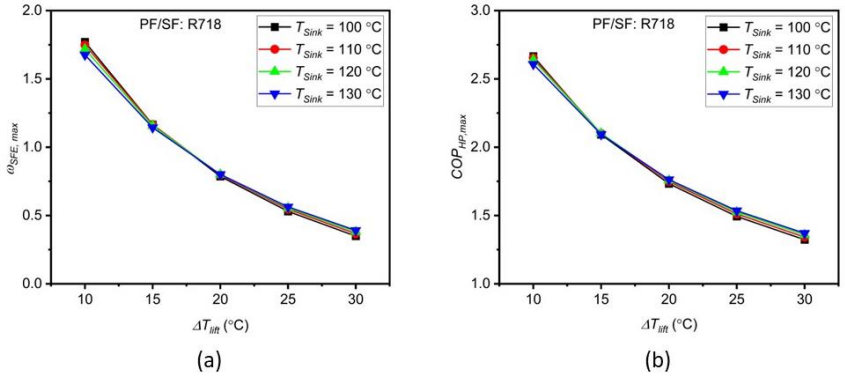

Fig. 6. The maximum performance of SFEs and SFE HTHPs with R718. (a) Maximum entrainment ratio and (b) maximum COP.

4.3. Comparison of BFEs and SFEs

Figure 7 compares the performance of ejectors and ejector HTHPs with single and binary fluids. Generally, ω_{max} of the BFEs was much lower than that of SFEs, but $COP_{HP,max}$ of BFE HTHPs was comparable to that of SFE HTHPs. For SFEs, HFE7500 has larger $\omega_{SFE,max}$ but smaller $COP_{HP,max}$ than R718. The discrepancy in $\omega_{SFE,max}$ and $COP_{HP,max}$ is due to the difference in changed specific enthalpy of the PF in the HTE, Δh_{PF}, and the SF in the LTE, Δh_{SF}. The binary fluids have a much larger $\Delta h_{SF}/\Delta h_{PF}$ but a much smaller $\omega_{SFE,max}$, as described in Table 3. According to Eq. (1), $COP_{HP,max}$ is linearly related to the product of $\omega_{SFE,max}$ and $\Delta h_{SF}/\Delta h_{PF}$. Therefore, BFE HTHPs and SFE HTHPs had comparable values of $COP_{HP,max}$. SFEs with R718 provided the best performance of HTHPs at a low ΔT_{lift}, whereas BFEs with HFE7500/R718 only provided a slightly better performance of HTHPs at ΔT_{lift} > 25°C. This indicates that selecting HFE7500/R718 as a binary-fluid pair for BFE HTHPs cannot fully extract the technical potential of BFE HTHPs. Considering the system

simplification of ejector HTHPs, SFEs with R718 are recommended for heat-driven ejector HTHPs. In addition, operating a SFE HTHP with R718 in an open-loop system may improve $\omega_{SFE,max}$.

For SFE HTHPs with R718 operated at T_{sink} = 120°C and ΔT_{lift} = 10°C–30°C, Carnot efficiencies (i.e., the second law efficiencies) ranged from 6.7% to 10.4%, which are much lower than those of conventional HTHPs—typically 40%–60% from experimental measurements [29].

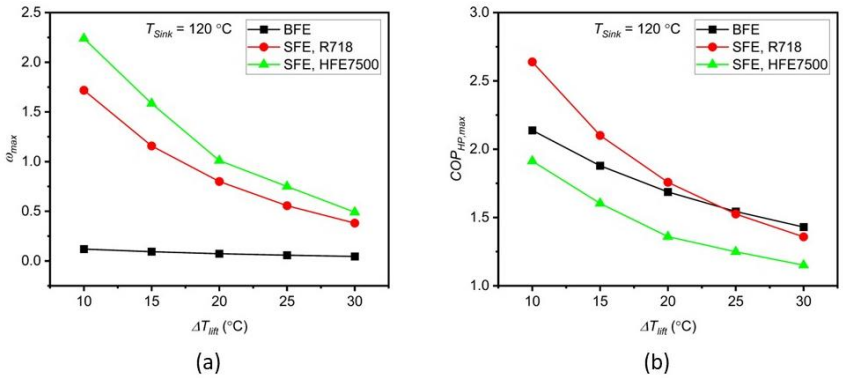

Fig. 7. Comparation of BFE HTHPs and SFE HTHPs. (a) Maximum entrainment ratio and (b) maximum COP.

Table 3. Working fluids for heat-driven ejector HTHPs

Ejectors	PF-SF	T_{HTE} (°C)	T_{sink} (°C)	ΔT_{lift} (°C)	$\Delta h_{SF}/\Delta h_{PF}$	ω	COP_{HP}
BFE	HFE7500-R718	240	120	10	9.50	0.12	2.14
SFE	HFE7500	230	120	10	0.41	2.24	1.91
SFE	R718	260	120	10	0.95	1.72	2.64

5. Conclusions

This study explored the technical potential of heat-driven ejector HTHPs. SFEs and BFEs were theoretically evaluated regarding the performance of ejector HTHPs. The entrainment ratios of ejectors were predicted with a geometry-free model. A thermodynamic model of an ejector HTHP was developed with mass and energy conservation equations. HFE7500 and R718 were selected as the working fluids for SFEs and BFEs. The performance of ejector HTHPs was investigated under the operation of T_{sink} = 100°C–130°C and ΔT_{lift} = 10°C–30°C. The conclusions from this primary study are as follows:

- SFEs had better component-level performance than BFEs in terms of the entrainment ratio, and BFEs had a much smaller entrainment ratio than SFEs.
- HTHPs with BFEs and SFEs had comparable heating cycle performance.
- The binary-fluid pair of HFE7500 and R718 cannot fully extract the technical potential of BFEs. An SFE with R718 could be a candidate for heat-driven ejector HTHPs.
- The Carnot efficiency of heat-driven ejector HTHPs was much lower than the state-of-the-art electric-driven HTHPs

Future research will focus on

- Seeking binary-fluid pairs for BFEs to provide a large entrainment ratio and a large difference in the increased enthalpy in the HTE and LTE; and
- Identifying the deployment of steam ejector HTHPs in open-loop applications.

NOMENCLATURE

BFE	binary-fluid ejector	(-)
COP	coefficient of performance	(-)
COND	condenser	(–)

EJT	ejector	(-)
GWP	global warming potential	(-)
h	enthalpy	(kJ/kg)
HTE	high-temperature evaporator	(-)
HTHP	high-temperature heat pump	(-)
LTE	low-temperature heat pump	(-)
MW	molecular weight	(kg/kmol)
$\dot{m}$	mass flow rate	(kg/s)
NBP	normal boiling point	(°C)
PF	primary fluid	(-)
Q	thermal capacity	(kW)
T	temperature	(°C)
SEP	separator	(–)
SFE	single-fluid ejector	(–)
SF	secondary fluid	(–)
W	power	(kJ/kg)

Symbol

ω	entrainment ratio	(-)
ρ	density	(kg/m^3)
η	component efficiency	(-)
x	quality of vapor	(-)

Subscript

lv	latent heat of evaporation
opt	optimum
max	maximum
i, ii, iii, . . .	state points within an ejector
1, 2, 3, . . .	state points within the loop of ejector heat pumps

Acknowledgements

This work was sponsored by the US Department of Energy's Building Technologies Office under contract no. DE-AC05-00OR22725 with UT-Battelle LLC. The authors would like to acknowledge the technology manager, Mr. Antonio Bouza, for his support.

References

[1] C. Mateu-Royo, C. Arpagaus, A. Mota-Babiloni, J. Navarro-Esbrí, and S. S. Bertsch, "Advanced high temperature heat pump configurations using low GWP refrigerants for industrial waste heat recovery: A comprehensive study," *Energy Conversion and Management*, vol. 229, p. 113752, 2021/02/01/ 2021, doi: https://doi.org/10.1016/j.enconman.2020.113752.

[2] G. Kosmadakis, C. Arpagaus, P. Neofytou, and S. Bertsch, "Techno-economic analysis of high-temperature heat pumps with low-global warming potential refrigerants for upgrading waste heat up to 150 °C," *Energy Conversion and Management*, vol. 226, p. 113488, 2020/12/15/ 2020, doi: https://doi.org/10.1016/j.enconman.2020.113488.

[3] Y. He, F. Cao, L. Jin, X. Wang, and Z. Xing, "Experimental study on the performance of a vapor injection high temperature heat pump," *International journal of refrigeration*, vol. 60, pp. 1-8, 2015.

[4] G. F. Frate, L. Ferrari, and U. Desideri, "Analysis of suitability ranges of high temperature heat pump working fluids," *Applied Thermal Engineering*, vol. 150, pp. 628-640, 2019.

[5] C. Arpagaus and S. Bertsch, "Experimental Comparison of HCFO and HFO R1224yd (Z), R1233zd (E), R1336mzz (Z), and HFC R245fa in a High Temperature Heat Pump up to 150 C Supply

Temperature," presented at the International Refrigeration and Air Conditioning Conference. , 2021, 1875.
[6] J. M. Pinheiro, S. Salústio, J. Rocha, A. A. Valente, and C. M. Silva, "Adsorption heat pumps for heating applications," *Renewable and Sustainable Energy Reviews*, vol. 119, p. 109528, 2020/03/01/ 2020, doi: https://doi.org/10.1016/j.rser.2019.109528.
[7] Q. Chen, M. Yu, G. Yan, and J. Yu, "Thermodynamic analyses of a modified ejector enhanced dual temperature refrigeration cycle for domestic refrigerator/freezer application," *Energy*, p. 122565, 2021/11/06/ 2021, doi: https://doi.org/10.1016/j.energy.2021.122565.
[8] A. Abu-Heiba, "Literature Review of Potential Thermally Activated Heat Pump Cycles," United States, 2018. [Online]. Available: https://www.osti.gov/biblio/1480616. https://www.osti.gov/servlets/purl/1480616
[9] S. Elbel and P. Hrnjak, "Ejector refrigeration: an overview of historical and present developments with an emphasis on air-conditioning applications," presented at the International Refrigeration and Air Conditioning Conference, 2008, 884.
[10] S. Elbel and N. Lawrence, "Review of recent developments in advanced ejector technology," *International Journal of Refrigeration*, vol. 62, pp. 1-18, 2016/02/01/ 2016, doi: https://doi.org/10.1016/j.ijrefrig.2015.10.031.
[11] Y. Fang, S. Croquer, S. Poncet, Z. Aidoun, and Y. Bartosiewicz, "Drop-in replacement in a R134 ejector refrigeration cycle by HFO refrigerants," *International Journal of Refrigeration*, vol. 77, pp. 87-98, 2017/05/01/ 2017, doi: https://doi.org/10.1016/j.ijrefrig.2017.02.028.
[12] J. Zheng, Y. Hou, Z. Tian, H. Jiang, and W. Chen, "Simulation Analysis of Ejector Optimization for High Mass Entrainment under the Influence of Multiple Structural Parameters," *Energies*, vol. 15, no. 19, p. 7058, 2022. [Online]. Available: https://www.mdpi.com/1996-1073/15/19/7058.
[13] F. Riaz, P. S. Lee, and S. K. Chou, "Thermal modelling and optimization of low-grade waste heat driven ejector refrigeration system incorporating a direct ejector model," *Applied Thermal Engineering*, vol. 167, p. 114710, 2020.
[14] K. Braimakis, "Solar ejector cooling systems: A review," *Renewable Energy*, vol. 164, pp. 566-602, 2021/02/01/ 2021, doi: https://doi.org/10.1016/j.renene.2020.09.079.
[15] D. Buyadgie, O. Buyadgie, S. Artemenko, A. Chamchine, and O. Drakhnia, "Conceptual design of binary/multicomponent fluid ejector refrigeration systems," *International Journal of Low-Carbon Technologies*, vol. 7, no. 2, pp. 120-127, 2012.
[16] P. Wang, H. Ma, J. Spitzenberger, A. Abu-Heiba, and K. Nawaz, "Thermal performance of an absorption-assisted two-stage ejector air-to-water heat pump," *Energy Conversion and Management*, vol. 230, p. 113761, 2021.
[17] M. El Hassan, "Numerical Characterization of the Flow Dynamics and COP Estimation of a Binary Fluid Ejector Ground Source Heat Pump Cooling System," *Fluids*, vol. 7, no. 7, p. 250, 2022.
[18] O. Drakhnia, D. I. Buyadgie, T. Miyazaki, O. D. Buyadgie, G. Herrera, and A. Chamchine, "Binary Fluids Application In The Ejector Energy Systems," in *ASTFE Digital Library*, 2017: Begel House Inc.
[19] D. Oleksii, T. Miyazaki, B. Olexiy, B. Dmytro, and A. Sergei, "Fractionating Condenser for Binary Fluid Ejector Refrigerating System," presented at the International Exchange and Innovation Conference on Engineering & Science(IEICES), Kyushu University, Japan, 2017.
[20] J. Spitzenberger, P. Wang, L. Ismael, H. Ma, A. Abuheiba, and K. Nawaz, "Theoretical Analysis of a Single-Stage Gas-Fired Ejector Heat Pump Water Heater," *Journal of Thermal Science and Engineering Applications*, vol. 14, no. 4, p. 041009, 2021.
[21] D. A. Pounds, J. Dong, P. Cheng, and H. Ma, "Experimental investigation and theoretical analysis of an ejector refrigeration system," *International Journal of Thermal Sciences*, vol. 67, pp. 200-209, 2013.
[22] I. W. Eames, S. Aphornratana, and H. Haider, "A theoretical and experimental study of a small-scale steam jet refrigerator," *International Journal of Refrigeration*, vol. 18, no. 6, pp. 378-386, 1995/07/01/ 1995, doi: https://doi.org/10.1016/0140-7007(95)98160-M.
[23] B. Huang, J. Chang, C. Wang, and V. Petrenko, "A 1-D analysis of ejector performance," *International journal of refrigeration*, vol. 22, no. 5, pp. 354-364, 1999.
[24] G. J. Sherwood, "Hydrofluoroethers as low temperature refrigerants," ed: Google Patents, 1998.

[25] J. G. Owens, "Low GWP alternatives to HFCs and PFCs," in Proceedings of the 1999 Taipei International Conference on Atmosphere Protection, 1999.
[26] J. Dong, X. Chen, W. Wang, C. Kang, and H. Ma, "An experimental investigation of steam ejector refrigeration system powered by extra low temperature heat source," *International Communications in Heat and Mass Transfer,* vol. 81, pp. 250-256, 2017/02/01/ 2017, doi: https://doi.org/10.1016/j.icheatmasstransfer.2016.12.022.
[27] J. Spitzenberger *et al.*, "Experimental performance of ejector heat pump operating in the sub-critical mode," *Energy Conversion and Management,* vol. 278, p. 116724, 2023.
[28] D.-W. Sun, "Comparative study of the performance of an ejector refrigeration cycle operating with various refrigerants," *Energy conversion and management,* vol. 40, no. 8, pp. 873-884, 1999.
[29] C. Arpagaus, F. Bless, M. Uhlmann, J. Schiffmann, and S. S. Bertsch, "High temperature heat pumps: Market overview, state of the art, research status, refrigerants, and application potentials," *Energy,* vol. 152, pp. 985-1010, 2018/06/01/ 2018, doi: https://doi.org/10.1016/j.energy.2018.03.166.